Photoinduced Electron Transfer in a Protein−Surfactant Complex: Probing the Interaction of SDS with BSA

Anjan Chakraborty, Debabrata Seth, Palash Setua, and Nilmoni Sarkar*

Department of Chemistry, Indian Institute of Technology, Kharagpur 721 302, WB, India

Received: March 14, 2006; In Final Form: June 21, 2006

Photoinduced fluorescence quenching electron transfer from *N*,*N*-dimethyl aniline to different 7-amino coumarin dyes has been investigated in sodium dodecyl sulfate (SDS) micelles and in bovine serum albumin (BSA)−SDS protein−surfactant complexes using steady state and picosecond time resolved fluorescence spectroscopy. The electron transfer rate has been found to be slower in BSA−SDS protein−surfactant complexes compared to that in SDS micelles. This observation has been explained with the help of the "necklace-and-bead" structure formed by the protein−surfactant complex due to coiling of protein molecules around the micelles. In the correlation of free energy change to the fluorescence quenching electron transfer rate, we have observed that coumarin 151 deviates from the normal Marcus region, showing retardation in the electron transfer rate at higher negative free energy region. We endeavored to establish that the retardation in the fluorescence quenching electron transfer rate for coumarin 151 at higher free energy region is a result of slower rotational relaxation and slower translational diffusion of coumarin 151 (C-151) compared to its analogues coumarin 152 and coumarin 481 in micelles and in protein−surfactant complexes. The slower rotational relaxation and translational diffusion of C-151 are supposed to be arising from the different location of coumarin 151 compared to coumarin 152 and coumarin 481.

1. Introduction

The interaction of proteins with surfactants has received a great deal of interest for many years due to its application in a great variety of industrial, biological, and cosmetics systems.[1−7] The globular protein bovine serum albumin (BSA) has the important role of interacting with cell membrane surfactant. BSA functions biologically as a career for fatty acid anions and other simple amphiphiles in a blood stream. It has a molecular weight of 66 411 g mol^{-1} and contains 583 amino acids in a single polypeptide chain. The protein contains 17 disulfide bridges and one free −SH group, which can cause it to form a covalently linked dimer. At neutral pH, it undergoes conformational changes. The interior of the protein is almost hydrophobic, while both the charged amino acid residues and apolar patches cover the interface.[8−10]

It is known in general that anionic surfactants interact strongly with the proteins and form protein−surfactant complexes.[4−7] This leads to the unfolding of proteins. The binding isotherm of BSA with surfactant is well studied.[4−6] It consists of four regions with increasing surfactant concentration. At the initial region, surfactant binds to the specific high-energy region of the protein. The concentration of the surfactant is the lowest at this region. The second region is the noncooperative interaction. The third region corresponds to the massive increase in binding due to the cooperative ligand interaction. The unfolding of proteins is believed to start in this region. Here, the "necklace-and-bead" structure of BSA−surfactant begins to form. The last region is associated with a growth in protein bound micelles, and further binding of the surfactant to the protein does not occur.[1−7] Several techniques such as X-ray crystallography,[11] NMR,[4,12,13] light scattering,[14−17] and small angle neutron scattering (SANS)[18,19] have been used to unravel protein−surfactant interaction. Different photophysical[20−22] and dynamical[23−26] studies have also been employed to probe the protein−surfactant interaction.

SCHEME 1: Structures of the Coumarin Dyes and Aromatic Amine

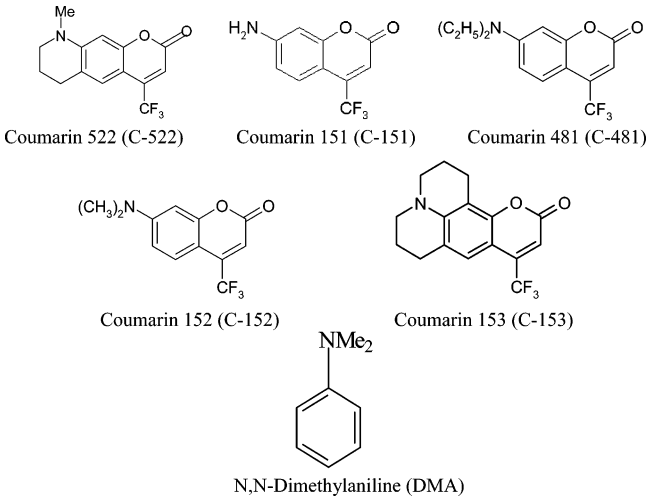

In this work, we are going to explore the fluorescence quenching electron transfer (ET) dynamics in sodium dodecyl sulfate (SDS) micelles and in BSA−SDS protein−surfactant complexes using steady state and picosecond time resolved fluorescence spectroscopy. We have used several coumarin dyes as the electron acceptors and *N*,*N*-dimethylaniline (DMA) as the donor (Scheme 1). Several groups[4−7,15,16] have studied the interactions between BSA and SDS. Takeda et al.[15] reported

* To whom correspondence should be addressed. E-mail: nilmoni@chem.iitkgp.ernet.in. Fax: 91-3222-255303.

10.1021/jp0615860 CCC: $33.50
Published on Web 07/29/2006

SCHEME 2: Necklace-and-Bead Structure of BSA−SDS Complexes Containing Bulk and Bound Water

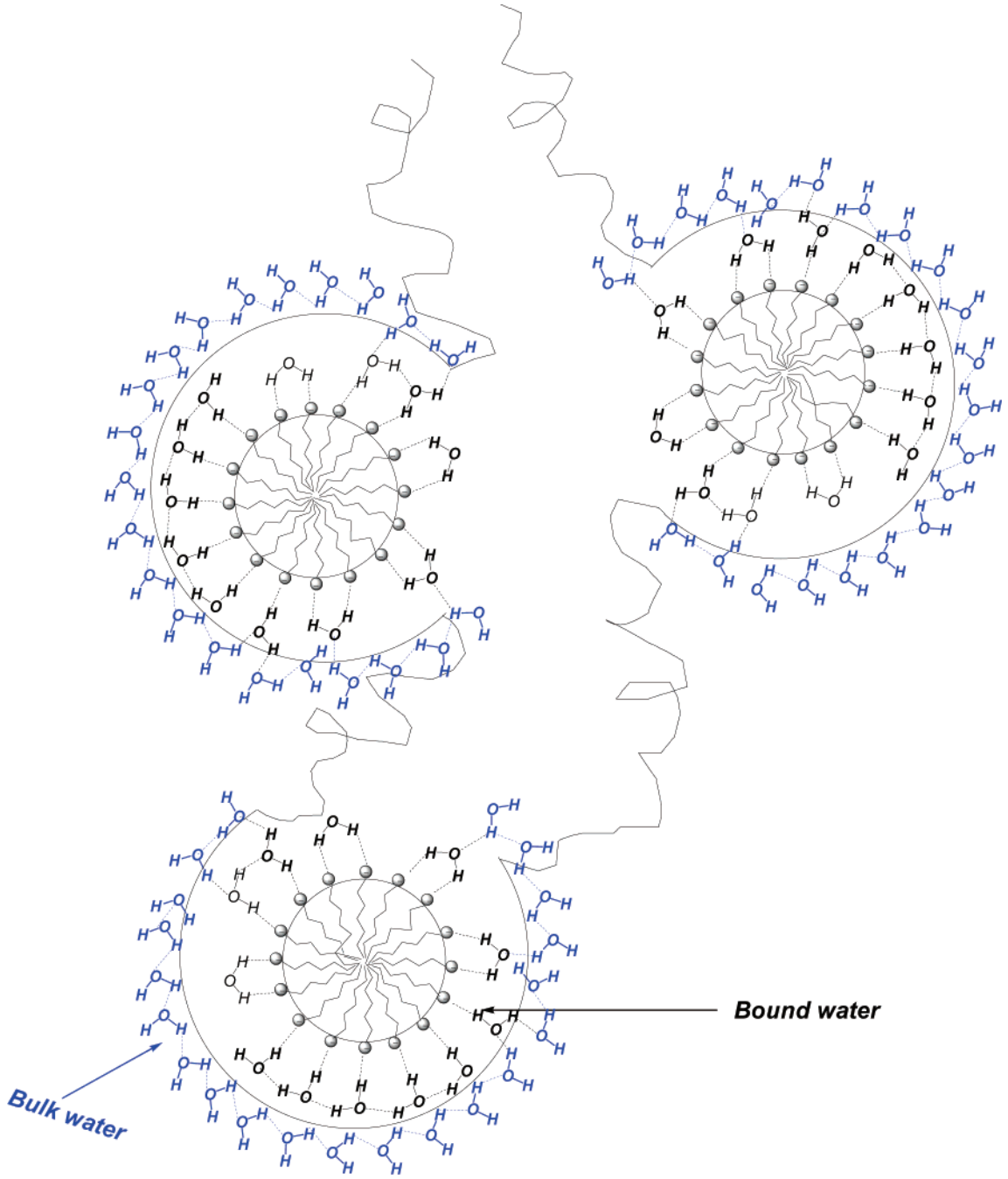

that above an SDS concentration of 8 mM, that is, at the saturated region of the binding isotherm, the radius of the BSA−SDS protein−surfactant complex is around 6 nm. Valstar et al.[16] reported that the hydrodynamic radius of BSA−SDS protein−surfactant complexes varies from 3.39 nm at [SDS] = 0 to around 6 nm at [SDS] = 7 mM. They found that the saturated binding for anionic surfactant (SDS) is pH independent, and their estimated hydrodynamic radius is comparable to that found by Takeda et al. Recently, Turro et al.[4] studied BSA−SDS complexes using electron spin resonance (ESR) and NMR techniques. They proposed a necklace-and-bead structure for BSA−SDS complexes. Valstar et al. latter on reported a necklace-and-bead structure for BSA−SDS and lysozyme−SDS complexes.[20] The necklace-and-bead structure is illustrated in Scheme 2. According to this scheme, at the saturated region of the binding isotherm, the BSA coils around the SDS micelles and results in an increase in the overall radius. Earlier, we reported[23] solvation dynamics in SDS micelles and in BSA−SDS protein−surfactant complexes. It was found that solvation dynamics is several times slower in BSA−SDS complexes compared to that in protein free SDS micelles. The slowing down of solvation dynamics[23] in BSA−SDS complexes compared to that in SDS micelles was attributed to the necklace-and-bead structure formed by the potein−surfactant complex. Thus, it would be interesting to carry out fluorescence quenching electron transfer in SDS micelles and in BSA−SDS protein−surfactant complexes.

There are many reports available in the literature regarding photoinduced electron transfer and back electron transfer in pure solution using different donors such as aniline, *N*,*N*-dimethylaniline, and so forth, and acceptors such as nile blue, oxazin, and oxazin-1.[27−33] In the present case, we used several 7-amino coumarin dyes and *N*,*N*-dimethylaniline (DMA) to investigate fluorescence quenching electron transfer studies. The previous

reports[34−42] suggest that the fluorescence quenching of coumarin dyes occurs due to electron transfer from DMA to excited dye molecules. According to Marcus theory,[43−45] the electron transfer rate increases with an increase in the negative free energy change of the system, reaches a maximum at some intermediate negative free energy, and then falls off at a higher negative free energy region. The present case represents a bimolecular electron transfer reaction; hence, diffusion would be the rate-determining step. Therefore, the observed electron transfer rate, that is, the rate of quenching, should be maximum to the diffusion limit. Thus, we should observe saturation in the electron transfer rate when this is correlated to the free energy change of the system. However, there are reports[46−51] where at higher negative free energy region electron transfer has been found to be retarded, apparently looking like an inversion, which is very unlikely in a bimolecular electron transfer reaction. Recently, we reported fluorescence quenching electron transfer from DMA to coumarin dyes in DTAB micelles and in BSA−DTAB protein−surfactant complexes.[52] It was shown by us that retardation in the electron transfer rate at higher free energy change (i.e., inversion) occurs only in the case of coumarin 151 (C-151) and the factors responsible for such behavior for C-151 are slower rotational relaxation and slower translational diffusion of C-151 compared to its analogue dyes C-152 and C-481. In the present work, we endeavored to strengthen our earlier work to establish the fact that the appearance of a Marcus inverted region in a micellar medium is a consequence of the slower rotational relaxation and hence the slower translational diffusion of C-151 compared to those of its analogues C-152 and C-481.

2. Experimental Section

All of the coumarin dyes were obtained from Exciton (laser grade) and used as received. *N*,*N*-Dimethylaniline (DMA) was obtained from Aldrich and distilled under reduced pressure just before use. The structures of the coumarin dyes and DMA are shown in Scheme 1. SDS was obtained from Aldrich. BSA was obtained from Sigma. All of the solutions were prepared in phosphate buffer solution at pH 5.6 according to Almgren et al.[20] The ionic strength of the buffer medium was adjusted to 0.2 M. The concentration of SDS was 50 mM in the corresponding micelles. The BSA−SDS complex was prepared by adding 200 mg of BSA (1%) and 290 mg of SDS (50 mM) to 20 mL of buffer solution at pH 5.60. The solution was then allowed to gently mix for about 5−6 h. The coumarins were initially dissolved in methanol. The saturated methanol solution of coumarins (3 μL) was added to dry quartz cuvettes. It was given sufficient time to ensure that all the methanol solution had been removed at room temperature. A 3 mL portion of BSA−SDS solution was then added to each cuvette and stirred very gently. The steady state absorption and emission spectra were recorded using a Shimadzu (model no UV-1601) UV−vis absorption spectrophotometer and a Jobin Yvon Fluoromax-3 spectrofluorimeter. The details of the picosecond time resolved fluorescence spectrophotometer were described elsewhere.[23] Briefly, we used a picosecond diode laser (IBH, UK) at 408 nm. The signal was detected at magic angle (54.7°) polarization using a Hamamatsu MCP PMT (3809U). The time resolution of our experimental setup was ~90 ps. For anisotropy measurements, we used the same setup. For the anisotropy measurements, the emission intensities at parallel ($I_{||}$) and perpendicular ($I_{\perp}$) polarizations were collected alternatively until a certain peak difference between parallel ($I_{||}$) decay and perpendicular ($I_{\perp}$) decay was reached. The peak difference depended on the tail matching of the parallel ($I_{||}$) and perpendicular ($I_{\perp}$) decays. The analysis of the data was done using IBH DAS 6 decay analysis software. The same software was also used to analyze the anisotropy data.

The temperature was maintained at 298 ± 1 K for all measurements.

TABLE 1: Absorption and Emission Maxima of Coumarin Dyes in SDS Micelles and in BSA−SDS Complexes (Solution Prepared in Phosphate Buffer (pH 5.6, Ionic Strength 0.2 M))

system	λ_{abs}^{max} (nm)	λ_{emi}^{max} (nm)
water + C-151	364	492
water + C-152	403	526
water + C-481	412	527
water + C-522	420	532
water + C-153	435	549
50 mM SDS + C-151	381	485
50 mM SDS + C-152	408	516
50 mM SDS + C-481	414	511
50 mM SDS + C-522	423	520
50 mM SDS + C-153	436	538
50 mM SDS−1% BSA + C-151	378	483
50 mM SDS−1% BSA + C-152	408	511
50 mM SDS−1% BSA + C-481	408	506
50 mM SDS−1% BSA + C-522	421	518
50 mM SDS−1% BSA + C-153	435	534

3. Results and Discussion

3A. Steady State Absorption and Emission Spectra. The steady state absorption spectra were measured in water, SDS micelles, and in BSA−SDS protein−surfactant complexes. The absorption peak maxima are listed in Table 1. It is revealed from Table 1 that the absorption peaks of C-152, C-481, C-522, and C-153 remain unchanged upon going from pure water to SDS micelles and BSA−SDS protein−surfactant complexes. However, the absorption peak of C-151 is found to be vastly red shifted from pure water to SDS micelles. In pure water, C-151 has an absorption peak at around 364 nm; it becomes 380 nm in SDS micelles and in BSA−SDS protein−surfactant complexes. The red shift for C-151 may originate from the ground state interaction between C-151 and the polar headgroup of the surfactant. The emission peak maxima are listed in Table 1. The emission maxima of coumarin dyes are found to be blue shifted in SDS micelles and in protein and BSA−SDS protein−surfactant complexes compared to pure water. The quantum yields of coumarin dyes are also higher in these systems as compared to the pure water. The blue shift in the emission maxima of coumarin dyes in micelles, protein, and protein−surfactant complexes indicates that probe molecules feel a less polar environment in these systems compared to that in water. The large blue shift of coumarin molecules in protein solution indicates that the interior of the protein molecule is much more hydrophobic than the protein−surfactant complex. It is possible that coumarin dyes may reside inside the hydrophobic pocket of protein for which a large blue shift appears in the emission spectra. The larger blue shift in BSA−SDS protein−surfactant complexes compared to SDS micelles indicates that the environment in BSA−SDS protein−surfactant complexes is less polar than that in SDS micelles. Again, the smaller blue shift in protein−surfactant complexes compared to pure protein solution indicates that protein goes to a denatured state upon addition of surfactant.

3B. Time Resolved Anisotropy Measurement. Absorption and emission spectra give only a qualitative idea regarding the location of the probe. For better insight regarding the location of the probe, we carried out time resolved anisotropy measure-

TABLE 2: Initial Anisotropy (r_0) and Rotational Relaxational Times of Coumarin Dyes in SDS Micelles and in SDS−BSA Complexes (Solution Prepared in Phosphate Buffer (pH 5.6, Ionic Strength 0.2 M))

system	r_0	a_{1r} (%)	τ_{1r} (ns)	a_{2r} (%)	τ_{2r} (ns)	$\langle\tau_r\rangle^a$ (ns)
water + C-151	0.40					0.100
water + C-152	0.39					0.120
water + C-481	0.40					0.130
water + C-522	0.40					0.120
water + C-153	0.40					0.100
50 mM SDS + C-151	0.28	0.730	0.26	0.27	1.486	0.590
50 mM SDS + C-152	0.33	0.460	0.126	0.54	0.600	0.380
50 mM SDS + C-481	0.33	0.400	0.190	0.60	0.640	0.450
50 mM SDS + C-522	0.29	0.470	0.157	0.53	0.775	0.485
50 mM SDS + C-153	0.22	0.79	0.387	0.21	1.645	0.650
50 mM SDS−1% BSA + C-151	0.37	0.540	0.281	0.460	2.110	1.121
50 mM SDS−1% BSA + C-152	0.29	0.380	0.107	0.620	1.000	0.660
50 mM SDS−1% BSA + C-481	0.24	0.58	0.200	0.42	1.450	0.725
50 mM SDS−1% BSA + C-522	0.33	0.57	0.316	0.43	1.805	0.956
50 mM SDS−1% BSA + C-153	0.32	0.545	0.431	0.455	2.319	1.290

[a] Error in the result ±5%.

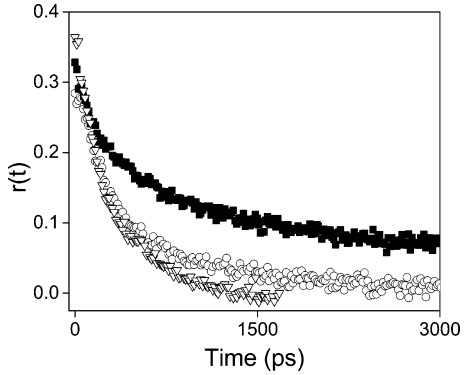

Figure 1. Fluorescence anisotropy decays ($r(t)$) of C-151 in BSA−SDS complexes (■) and fluorescence anisotropy decays of C-151 (○) and C-152 (▽) in SDS micelles. Solution prepared in phosphate buffer (pH 5.6, ionic strength 0.2 M).

ments of coumarin dyes in pure water, SDS micelles (50 mM), and BSA (1%)−SDS (50 mM) protein−surfactant complexes prepared in phosphate buffered solution at pH 5.6, ionic strength 0.2 M. The anisotropy decay ($r(t)$) is expressed as

$$r(t) = \frac{I_{||}(t) - GI_{\perp}(t)}{I_{||}(t) + 2GI_{\perp}(t)} \quad (1)$$

where $I_{||}(t)$ and $I_{\perp}(t)$ are fluorescence decays polarized parallel and perpendicular to the polarization of the excitation light, respectively. The G factor is 0.6 in our experimental setup. The time correlated rotational anisotropy function was fitted biexponentially as

$$r(t) = r_0[a_{1r}\exp(-t/\tau_{fast}) + a_{2r}\exp(-t/\tau_{slow})] \quad (2)$$

The fitted results of time resolved anisotropy decays for all the dyes in pure water, SDS micelles, and SDS−BSA protein−surfactant complexes are summarized in Table 2. The representative anisotropy decays of C-151 and C-152 in SDS micelles and anisotropy decay of C-151 in BSA−SDS complexes are shown in Figure 1.

It is revealed from Table 2 that coumarin dyes have much longer rotational relaxation times in micelles, protein solution, and protein−surfactant complexes as compared to that in pure water. Earlier, we reported[52] that the coumarin dyes have rotational relaxation times (Table 2) around 100 ps in pure water. This time constant of rotational relaxation is a little longer compared to the results reported by Shirota et al.[53,54] This may be attributed to the lower time resolution of our instrument compared to that used by Shirota et al. In pure water, anisotropy decays of coumarin dyes were fitted to a single-exponential function, while in SDS micelles and BSA (1%)−SDS (50 mM) protein−surfactant complexes the anisotropy decays were biexponential, consisting of a picosecond component and a nanosecond component. Thus, it may be concluded that in SDS micelles and in BSA (1%)−SDS (50 mM) protein−surfactant complexes coumarin molecules experience a more restricted environment compared to that in pure water. Earlier, we reported[23] that coumarin molecules in 1% BSA solution have a slow component of >3 ns. It may be possible that coumarin molecules in BSA are captured into the hydrophobic pocket where the rotational motion is drastically hindered compared to that in pure micelles. Thus, these exhibit a longer time resolution in pure BSA solution. The other striking observation is that in protein−surfactant complexes coumarin molecules exhibit a slower rotational relaxation than that in pure micelles. This may be explained in the following way.

We have chosen the saturated region of the binding isotherm of the BSA−SDS complex in which the protein is unfolded by the surfactant molecules.[4−6] It is already reported[4,20] that at this region some growth of protein bound micelle or necklace-and-bead structure is formed. It is reasonable that a long, flexible polypeptide chain wraps around the micellar aggregate (Scheme 1) formed and protects the probe from the bulk environment; hence, the mobility of the headgroup region is markedly hindered.[4,20] Thus, coumarin molecules show a slower rotational relaxation in protein−surfactant complexes compared to that in SDS micelles.

It is well-known[55−59] that the biexponential nature in anisotropy decay arises due to different types of rotations of the probe molecules inside the micellar surface. These motions are easily described by the two-step and wobbling-in-cone model. These two motions are coupled to the overall rotation of the micelles. According to these models,[55−59] the slow rotational relaxation time arises due to the lateral diffusion ($r_d(t)$) of the probe molecules at the interface of the micelles depending on its position and the fast relaxation time is a consequence of free wobbling ($r_w(t)$) of the probe molecules in a cone angle (θ_0). As these two motions are coupled to the overall rotation of micelles ($r_m(t)$), we may write the following equation

$$r(t) = r_w(t)\, r_d(t)\, r_m(t) \quad (3)$$

Again, we may write

$$r(t) = r_0[S^2 + (1 - S^2)\exp(-t/\tau_e)] \times \exp\{-t((1/\tau_d) + (1/\tau_m))\} \quad (4)$$

where r_0 denotes the initial anisotropy (i.e., at $t = 0$), τ_d and τ_e are the translation diffusion and wobbling motion of the dye molecules, and τ_m is the time for micellar rotation. S is the order parameter. The magnitude of S is a measure of spatial restriction and has values from zero (isotropic fast motion) to 1 (completely restricted motions). It is defined as

$$S^2 = a_{2r} \quad (5)$$

In the present case, the average S value is approximately 0.6−0.7. This indicates that probe molecules face a restricted environment inside the micellar surface. From the order parameter, the

TABLE 3: Analytical Rotational Parameters for Coumarins in SDS Micelles and SDS−BSA Protein−Surfactant Complexes (Solution Prepared in Phosphate Buffer (pH 5.6, Ionic Strength 0.2 M))

system	τ_m (ns)	τ_a (ns)	τ_e (ns)	τ_d (ns)	$D_w \times 10^{-8}$ (s^{-1})	$D_L \times 10^{-6}$ [a] (cm^2/s)
50 mM SDS + C-151	27		0.314	1.572	7.19	9.54
50 mM SDS + C-152	27		0.159	0.613	7.16	24.40
50 mM SDS + C-481	27		0.266	0.655	3.56	23.00
50 mM SDS + C-522	27		0.200	0.800	5.78	18.75
50 mM SDS + C-153	27		0.506	1.754	5.20	8.55
50 mM SDS−1% BSA + C-151	27	216	0.324	2.314	4.41	6.50
50 mM SDS−1% BSA + C-152	27	216	0.120	1.05	7.43	14.40
50 mM SDS−1% BSA + C-481	27	216	0.232	1.543	6.74	10.00
50 mM SDS−1% BSA + C-522	27	216	0.383	1.951	4.00	7.70
50 mM SDS−1% BSA + C-153	27	216	0.529	2.568	2.69	5.84

[a] Error in the result ±5%.

cone angle (θ_0, the cone angle in radians) has been derived from the following equation.

$$\theta_0 = \cos^{-1}\left[\frac{1}{2}((1+8S)^{1/2}-1)\right] \quad (6)$$

In the present case, we assume that the probe molecules are attached to the surface of the micelles. Therefore, the overall micellar rotation is obtained from the Stokes−Einstein Debye relation

$$\tau_m = \frac{4\pi\eta r_h^3}{3kT} \quad (7)$$

where η is the viscosity of water, r_h is the hydrodynamic radius of the micelles, and k and T are the Boltzmann constant and absolute temperature, respectively. For SDS micelles in the present case, τ_m is approximately 27 ns using a hydrodynamic radius of 30 Å.[60−62] According to Bhattacharyya et al.,[57] in a necklace-and-bead model, the polymer−surfactant aggregates consist of several beads of spherical micelles. Therefore, these micelles rotate inside the necklace, which is formed by the protein molecules (Scheme 1). In the present case, we assumed that SDS micelles have the same radius inside the necklace. Therefore, the τ_m value for the SDS micelles would be the same in the BSA−SDS protein−surfactant complexes. Again, after formation of a necklace-and-bead structure, the BSA−SDS complex will have a rotational motion ($r_a(t)$) along with the other motions with time constant τ_a. The motion of such aggregates was described by Bhattacharyya et al.[57] in the case of polymer−surfactant aggregates. Now, if the rotational motion (($r_a(t)$) of the overall BSA−SDS complex is taken into account, then eqs 3 and 4 become

$$r(t) = r_w(t)\, r_d(t)\, r_m(t)\, r_a(t) \quad (8)$$

$$r(t) = r_0[S^2 + (1-S^2)\exp(-t/\tau_e)] \times \exp\{-t((1/\tau_d) + (1/\tau_m) + (1/\tau_a))\} \quad (9)$$

where τ_a is the time for overall rotation of the BSA−SDS protein−surfactant complexes.

Therefore, the time for lateral diffusion (τ_d) is determined from the following equation

$$\frac{1}{\tau_d} = \frac{1}{\tau_{slow}} - \frac{1}{\tau_m} - \frac{1}{\tau_a} \quad (10)$$

and the wobbling time of the dye may be obtained from the following equitation

$$\frac{1}{\tau_e} = \frac{1}{\tau_{fast}} - \frac{1}{\tau_{slow}} \quad (11)$$

The lateral diffusion coefficient is defined as

$$D_L = \frac{r_h^2}{6\tau_D} \quad (12)$$

The radius of SDS micelles is well reported.[49,60−62] We already mentioned that the radius of BSA−SDS protein−surfactant complexes was reported to be around 6 nm by Almgren et al. and Takeda et al.[14−16] The value of τ_a for BSA−SDS complexes is found to be around 220 ns. As the value of τ_a is of the order of several nanoseconds and the fast and slow components of anisotropy decays are of the order of picoseconds, it has a negligible contribution to the lateral diffusion.

Now knowing all of the parameters, we may obtain the wobbling diffusion coefficient which is a consequence of the wobbling motion of the dye molecule in a cone

$$D_w = \frac{7\theta_0^2}{24\tau_e} \quad (13)$$

The anisotropy parameters are listed in Table 3.

3C. Fluorescence Quenching Studies of Coumarins by DMA. Previous reports[46−52,60] on electron transfer in micelles suggest that DMA prefers to stay at the micellar surface, that is, in the Stern layer of the micelles. DMA is sparingly soluble in water. However, its solubility increases dramatically in a micellar medium. Representative steady state fluorescence quenching spectra of C-153 in the presence of different concentrations of DMA in BSA−SDS protein−surfactant complexes are shown in Figure 2. It is found that there is no change in the shape of absorption spectra upon addition of DMA to the coumarin solution in SDS micelles and BSA−SDS protein−surfactant complexes. This indicates that no ground state complex formation occurs between the coumarin molecules and DMA. On the other hand, the emission spectra remain unaltered upon addition of DMA to the coumarin solution. Thus, it rules out the formation of any exciplex between DMA and coumarin molecules. We used the Stern−Volmer equation to estimate the fluorescence quenching electron transfer rate. The equation is as follows

$$\frac{I_0}{I} = 1 + K_{SV}[Q]_S \quad (14)$$

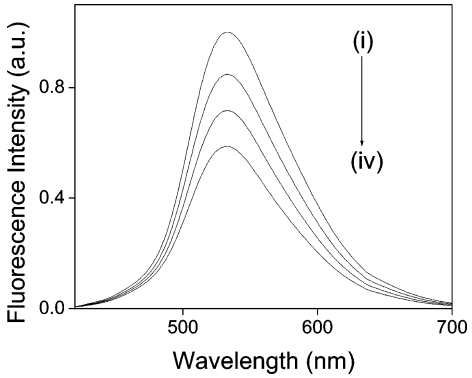

Figure 2. Steady state fluorescence quenching of C-153 in BSA−SDS complexes at DMA concentrations of (i) 0 M, (ii) 0.086 M, (iii) 0.172 M, and (iv) 0.258 M. Solution prepared in phosphate buffer (pH 5.6, ionic strength 0.2 M).

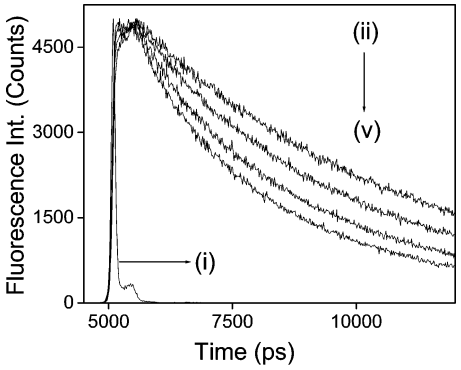

Figure 3. Time resolved fluorescence quenching decays of C-151 in BSA−DTAB complexes. Spectrum i is the instrument response, and spectra ii, iii, iv, and v are fluorescence transients at different DMA concentrations—0, 0.086, 0.172, and 0.258 M, respectively.

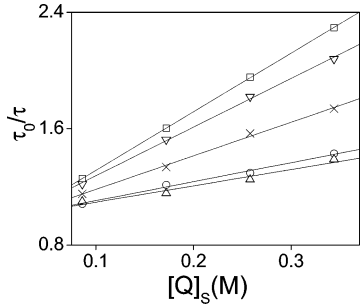

Figure 4. Stern−Volmer plots for (□) C-151, (○) C-152, (△) C-481, (▽) C-522, and (×) C-153 in BSA−SDS protein−surfactant complexes. Solution prepared in phosphate buffer (pH 5.6, ionic strength 0.2 M).

where I_0 and I are the intensity of the coumarin dyes in the absence and in the presence of the quencher. $[Q]_S$ is the concentration of DMA in the Stern layer of the micelles. This is calculated following the procedure reported elsewhere.[49−52] The radius of SDS micelles is well reported in the literature.[49,60−62] In the present work, phosphate buffer is used as the solvent instead of water; however, for the sake of simplicity, we have taken the radius of SDS reported earlier in the SANS study.[61,62] According to SANS study,[61,62] the hydrodynamic radius of SDS micelles is 3 nm and the radius of the hydrocarbon core is 2.1 nm. As SDS molecules bind to the all-available binding sites of BSA and form a necklace-and-bead structure, the radius of the BSA−SDS protein−surfactant complex increases significantly. Coumarin and DMA molecules preferably stay at the micellar surface, and the size of SDS aggregates in the necklace-and-bead structure remains close to that in SDS micelles. Thus, to a very good first approximation, it would be worthy to assume the same radius for SDS micelles and SDS aggregates forming a necklace-and-bead structure. The fluorescence quenching constant (k_Q) was determined by dividing the Stern−Volmer constant by the lifetime of the coumarin dyes in the absence of quencher. The results are summarized in Table 4. Similar to the steady state fluorescence quenching measurements, we carried out time resolved fluorescence quenching measurements to have a better understanding of the ET dynamics in these systems. Figure 3 shows the time resolved fluorescence quenching decays of coumarin 151 in BSA−SDS protein−surfactant complexes in the presence of different amounts of amine. It is seen that the lifetime gradually becomes shorter as the concentration of the amine increases. The quenching constant was determined by the following equations.

$$\frac{\tau_0}{\tau} = 1 + K_{SV}[Q]_S = 1 + k_Q\tau_0[Q]_S \qquad (15)$$

Typical plots for τ/τ_0 versus $[Q]_S$ in BSA−SDS protein−surfactant complexes are shown in Figure 4. The results are summarized in Table 4. It is important to note that the steady state fluorescence quenching constants (k_Q) are higher than that obtained from time resolved experiments. This comes from the static quenching in steady state experiment. Like our earlier reports,[52] here we also observed a slower fluorescence quenching electron transfer rate compared to that in an acetonitrile[63] medium or in neat amine solvent. In a homogeneous medium like acetonitrile, the donor and acceptor molecules are separated by the solvent molecules. The ion pair formed in this case after reaction is the solvent-separated ion pair (SSIP).[63] On the other hand, in micelles, incorporation of surfactant molecules increases the distance between donor and acceptor, causing a reduction

TABLE 4: Lifetime and Fluorescence Quenching Constants for Different Coumarin−Amine Systems in SDS Micelles and in BSA−SDS Complexes (Solution Prepared in Phosphate Buffer (pH 5.6, Ionic Strength 0.2 M))

system	wavelength (nm)	τ_0 (ns)	amine	SS[a] K_q (10^9 M^{-1} s^{-1})	TR[a] K_q (10^9 M^{-1} s^{-1})
50 mM SDS + C-151	485	5.77	DMA	1.68	1.00
50 mM SDS + C-152	516	0.921	DMA	3.27	2.02
50 mM SDS + C-481	511	0. 500	DMA	4.2	2.35
50 mM SDS + C-522	520	4.392	DMA	1.2	1.12
50 mM SDS + C-153	538	3.353	DMA	1.02	0.92
50 mM SDS−1% BSA + C-151	483	5.4	DMA	1.03	0.74
50 mM SDS−1% BSA + C-152	511	1.14	DMA	2.63	1.14
50 mM SDS−1% BSA + C-481	506	0.88	DMA	2.85	1.30
50 mM SDS−1% BSA + C-522	518	4.528	DMA	1.1	0.74
50 mM SDS−1% BSA + C-153	534	3.78	DMA	0.88	0.60

[a] Error in the result ±5%.

TABLE 5: Solvation Parameters of C-153 in SDS Micelles and BSA−SDS Protein−Surfactant Complexes

system	$\Delta\nu^*$ (cm^{-1})	a_1	τ_1 (ps)	a_2	τ_2 (ps)	$\langle\tau_s\rangle^a$ (ps)
50 mM SDS	304	0.93	153	0.07	470	175
50 mM SDS + 1% BSA	415	0.56	424	0.44	3870	600

[a] Error in the result ±5% (data taken from our earlier paper[23]).

in coupling strength between donor and acceptor; hence, the observed fluorescence quenching becomes slower. Another important observation is that the rate of quenching does not differ in SDS micelles from that in DTAB micelles. It is surprising because the solvation dynamics is faster in SDS micelles (∼175 ps) than that in DTAB (∼250 ps).[52] Thus, it is expected that the electron transfer rate in SDS micelles should be faster than that in DTAB micelles. Pal et al.[51] observed a much slower electron transfer rate in DTAB micelles than that in SDS micelles. This feature comes from the fact that in the present case phosphate buffer solution (pH 5.6, ionic strength 0.2 M) has been used for micelle formation. Due to the presence of counterions (from phosphate buffer), the repulsive interaction between the headgroups decreases and the micelles become more close-packed. This offers a better confinement to reactants, and thus, the acceptors and donor molecules are strongly entrapped by the surfactant molecules. Moreover, due to the presence of phosphate and sodium ions in the Stern layer, the occupancy number of the quencher per micelles decreases. The separation distance between the donor and acceptor molecules increases and results in a decrease in the electronic coupling strength. The increase in the distance by 1 Å between the donor and the acceptor decreases the electron transfer rate by an exponential factor. All of these facts together lead to a slower quenching rate in the present system than its expected value. Thus, we get a similar electron transfer rate in DTAB and SDS micelles, while a faster electron transfer rate is expected in SDS micelles. In this context, it would be interesting to compare the electron transfer rate in SDS micelles to that in BSA−SDS protein−surfactant complexes. It is revealed from Table 4 that the rate of fluorescence quenching is slower in BSA−SDS protein−surfactant complexes compared to that in SDS micelles. The experiment is carried out at the saturated region of the protein−surfactant binding isotherm. The protein is predominantly coiled around[4] the exterior micelles according to Scheme 1. The micelles like aggregates formed on the protein are more close-packed due to their smaller size than the corresponding micelles formed in protein free solution. In the necklace-and-bead structure (Scheme 1) of protein−surfactant complexes, it is reported that the headgroup region, that is, the Stern layer of micelles is squeezed due to wrapping up of the protein molecule around the micelles. Thus, the probe molecules experience a more confined geometry than protein free micelles, resulting in a decrease in the fluorescence quenching rate. The rotational relaxation studies and solvation dynamics studies[23] also support the fact that coumarin molecules face a more confined environment in protein−surfactant complexes than protein free micelles. In protein−surfactant complexes, the rotational relaxation times of coumarin molecules and solvation times have been found to be higher than those in protein free SDS micelles. The other important observation is that in pure BSA solution we did not observe a significant quenching. In our earlier publication, we reported this fact.[52] The rate of photoinduced eletron transfer depends on the spatial distribution of the donor molecules around an excited dye. In the present case, the high blue shift in emission spectra and high rotational relaxation time of coumarin molecules indicate that coumarin molecules are captured in the hydrophobic pocket in native BSA solution. Thus, they are inaccessible or very less accessible to the DMA molecules; hence, we observed a slow fluorescence quenching rate. Mazumdar et al.[64] reported that the binding site of the neutral probe PRODAN in the protein Tabulin is shielded from the solvent. In our earlier report[52] on electron transfer in DTAB micelles and in BSA−DTAB protein−surfactant complexes, we already mentioned that solvation dynamics was not observed in native BSA solution using C-153 as the probe.[23] Thus, solvation and rotational relaxation studies support this conjecture that coumarin molecules are buried inside the hydrophobic pockets in native BSA solution.

3D. Free Energy Change and Fluorescence Quenching. The electron transfer model used in the present case is based on the nonadiabatic condition. In this model, the solvent reorganization occurs on a much faster time scale compared to the electron transfer. However, in the present case, in SDS micelles and in BSA−SDS protein−surfactant complexes, solvation dynamics is competitive to the electron transfer rate or even slower. Thus, solvation dynamics contributes to the electron transfer dynamics. We recently reported[23] the solvation time in SDS micelles (175 ps) and in BSA−SDS protein−surfactant complexes (600 ps). Other groups reported solvation times in SDS micelles earlier.[54,65−68] The solvation dynamics is found to be slower in BSA−SDS protein−surfactant complexes than in SDS micelles. Earlier, we[52] reported a slower solvation in BSA−DTAB protein−surfactant complexes compared to DTAB micelles. The slowing down of solvation dynamics in BSA−SDS protein−surfactant complexes compared to protein free SDS micelles may be explained in the following way.

In the saturated region of the binding isotherm, the protein−surfactant complex protein promotes the formation of micelle-like aggregates by wrapping the polypeptide chain around the micelles; that is, a necklace-and-bead structure (Scheme 2) is

TABLE 6: Redox Potentials, E_{00} Values, and $\Delta G°$ Values for the Coumarin−Amine Systems Studied in SDS Micelles and SDS−BSA Complexes (Solution Prepared in Phosphate Buffer (pH 5.6, Ionic Strength 0.2 M))

system	E (A/A^-) (V) vs SCE[a]	E_{00} (eV)	amine	E (D/D^+) (V) vs SCE[a]	$\Delta G°$ (eV)
50 mM SDS + C-151	−1.565	2.840	DMA	0.756	−0.579
50 mM SDS + C-152	−1.626	2.680	DMA		−0.358
50 mM SDS + C-481	−1.660	2.680	DMA		−0.324
50 mM SDS + C-522	−1.653	2.623	DMA		−0.274
50 mM SDS + C-153	−1.685	2.537	DMA		−0.156
50 mM SDS−1% BSA + C-151	−1.565	2.857	DMA		−0.596
50 mM SDS−1% BSA + C-152	−1.626	2.720	DMA		−0.398
50 mM SDS−1% BSA + C-481	−1.660	2.732	DMA		−0.376
50 mM SDS−1% BSA + C-522	−1.653	2.634	DMA		−0.285
50 mM SDS−1% BSA + C-153	−1.685	2.558	DMA		−0.177

[a] Data taken from ref 34.

formed. However, no free micelles are available at this concentration. In the necklace-and-bead structure of protein−surfactant complexes, it may be possible that water molecules are squeezed between the peptide chain of protein and pure micelles and as a result the motion of water molecules becomes slower compared to pure micelles. Thus, the solvation dynamics becomes slower in protein−surfactant complexes compared to that in protein free SDS micelles. The slower solvation dynamics in BSA−SDS protein−surfactant complexes compared to that in pure SDS micelles leads to the slower electron transfer in BSA−SDS protein−surfactant complexes compared to that in protein free micelles.

Correlation of free energy change to the electron transfer rate yields several interesting results. According to Marcus theory,[43−45] the electron transfer rate is dependent on the free energy change of the system. Initially, with a negative change in free energy, the electron transfer rate increases, reaches a maximum, and then is retarded with further increase in negative free energy change. The last region is called the Marcus inverted region. In the present work, we have estimated the free energy change using the following equation

$$\Delta G = E_{ox} - E_{red} - E_{00} + \frac{e^2}{\epsilon_0 R} \tag{16}$$

Here, E_{00} is the energy difference between the S_0 and S_1 states. This was obtained from the intersecting wavelength of normalized fluorescence and normalized absorption spectra. E_{ox} and E_{red} denote the oxidation and reduction potentials of the donor and acceptor, respectively. We have used the standard value of oxidation and reduction potentials in an acetonitrile medium reported previously.[34] R is the distance between the donor and the acceptor. R is assumed to be the sum of the radii of the donors and the acceptors. The radii of the donor and acceptor molecules were estimated following Edward's[69] volume addition method assuming the molecules to be spherical. We have chosen a static dielectric constant (ϵ_0) of ~37.5, that is, the dielectric constant of the acetonitrile. Thus, the term $e^2/\epsilon_0 R$ has a value around 0.06 eV for all coumarin−amine systems. The results are summarized in Table 6.

As electron transfer between excited coumarin dyes and DMA molecules is a bimolecular reaction, the observed reaction rate constant has the form of a consecutive reaction mechanism consisting of diffusional (k_d) and activated (k_{act}) rate constants for electron transfer as follows

$$k_{obs} = \frac{k_{act} k_d}{k_{act} + k_d} \tag{17}$$

The above equation suggests that the observed rate constant (k_{obs}) would be equal to the diffusional (k_d) rate constant if diffusion is the rate-limiting step and the activated rate constant (k_{act}) is very high, that is, $k_{act} \gg k_d$. Consequently, the observed rate constants of most bimolecular reactions display an increase with increasing free energy followed by a leveling at the diffusional limit. The Marcus inverted region was observed in the case of a rigid system where intramolecular electron transfer occurs or in the case where a contact ion pair is formed.[70−73] The definitive confirmation of the existence of the Marcus inverted region in a truly intermolecular reaction was recently reported by a few groups.[74,75] Recently, Gopidas and coworkers[76,77] showed that the Marcus inverted region could be obtained in a series of donors and acceptors when these are hydrogen bonded. In the absence of hydrogen bonding, Rehm−

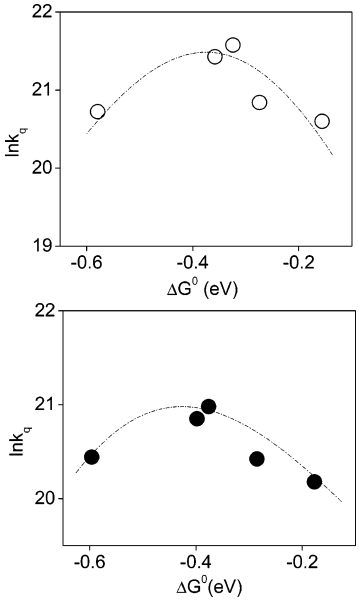

Figure 5. Plot of ln k_q vs $\Delta G°$ for the coumarin−DMA system in SDS micelles (○). Plot of ln k_q vs $\Delta G°$ for the coumarin−DMA system in BSA−SDS complexes (●). Solution prepared in phosphate buffer (pH 5.6, ionic strength 0.2 M). The short dashed line is used to guide a deviation in the Marcus curve at the higher free energy region.

Weller behavior was observed. In micelles, the Marcus inverted region was reported by our group and Kumbhakar et al. assuming the reactants are static in their position and no diffusion is taking place.[46,49−51] However, micelles are not completely rigid, so finite diffusion is possible. Fayer et al. emphasized the role of diffusion in micelles in several papers.[78,79] In micelles, it may be shown that the mean square displacement covered by an acceptor toward a donor by diffusion within the electron transfer time scale is >5 Å. Now, according to Marcus theory,[43−45] a change in the distance by 1 Å between donor and acceptor changes the electron transfer rate by an exponential factor. Thus, the role of diffusion in governing the electron transfer rate in micelles is very important.

In the present case, we observed retardation in the electron transfer rate at higher free energy region in correlation of free energy change to the electron transfer rate (Figure 5). The earlier reports[46,49−51] claimed such features as the Marcus inverted region. Careful investigation of the present work and previous reports reveals that retardation in the electron transfer rate at higher free energy change, that is, deviation from the normal Marcus region, occurs only in the case of C-151 in all of the cases. The interesting point is that the values of log P (an octanol−water partition coefficient, calculated using ChemDraw software) for C-151, C-152, C-481, C-522, and C-153 are 1.94, 2.99, 4.05, 3.66, and 4.08 and the value of DMA is 2.31. Thus, C-151 is the most hydrophilic dye and the hydrophobicities of C-151 and DMA are quite similar. This indicates that the distance between the DMA and a dye should be closer for C-151 than the other dyes. Therefore, the present observation does not merit an interpretation in terms of the donor/acceptor hydrophobicity. The other factors such as reorientation, diffusion, hydrogen bonding, and accessibility should be taken into account. In the following paragraph, we have tried to summarize all of these effects to arrive at a reasonable understanding for the present observation.

In steady state absorption spectra, C-151 exhibits a red shift, while for other coumarin dyes the absorption spectra remain unchanged. This is possible for C-151 if it forms a ground state complex with the surfactant molecules. This also indicates that

SCHEME 3: Location of Coumarin Dyes in Micelles, Bound Water, and Bulk Water

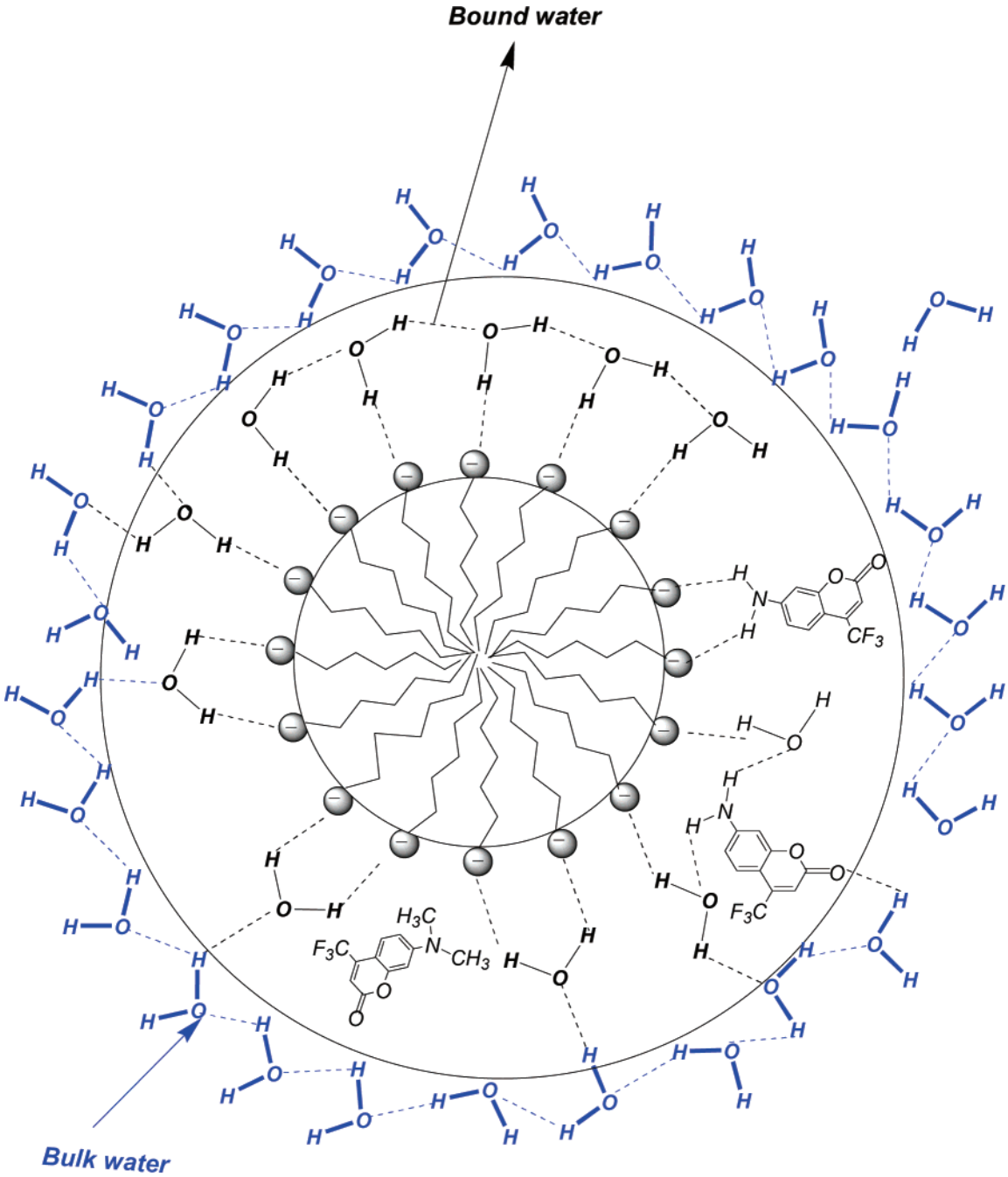

C-151 is strongly nucleated by the solvent molecules compared to other coumarin dyes. In the emission spectra, C-151 exhibits the least blue shift. Therefore, it is clear that C-151 is strongly nucleated by those solvent molecules which offer stronger hydrogen bonding to C-151 than other coumarin dyes. In the present situation, we speculate that C-151 molecules reside in closer proximity to the headgroup region than the other coumarin molecules because solvent molecules attached to the surfactant headgroups can make stronger hydrogen bonding to C-151 (Scheme 3). Recently, several reports[80,81] have been published where it has been shown that C-151 forms stronger hydrogen bonding than C-481 in hexane solution in the presence of different alcohols. The effect is ascribed to the nucleation of the hydrogen bonded cluster around the $-NH_2$ group. Recently, Das et al.[81] reported that C-151 has a greater tendency to form hydrogen bonds than its analogue C-500 in reverse micelles. They showed that the hydrogen bonding parameters are higher for C-151 than its analogue C-500. This implies that amino hydrogens of C-151 are responsible for stronger interaction with other molecules and this probability is reduced when amino hydrogen is replaced by one or more alkyl groups, which happened in the case of C-500.

In the present case, it appears in Figure 1 that C-151 shows a higher rotational relaxation time than its analogues C-152 and C-481. In SDS micelles, C-151 has a rotational relaxation time of 0.590 ns while C-152 and C-481 have rotational relaxation times of 0.380 and 0.450 ns, respectively. Earlier, we reported a similar observation in DTAB micelles. The unique feature of C-151 may be possible if C-151 experiences a different environment inside the micellar surface. Before going into any detailed discussion, let us have a look at the structural feature of micelles. Micelles are formed by aggregation of surfactant molecules in polar solvents above a certain concentration of the surfactant called the critical micellar concentration (cmc).

It consists of three regions, namely, the hydrocarbon core, the Stern layer, and the Gouychapman layer. The hydrocarbon core is composed of the hydrocarbon chain of the surfactant molecules. The second region is the Stern layer containing polar headgroups of the surfactant molecules, counterions, and solvent molecules. This layer is surrounded by the Gouychapman layer. As C-151 has a smaller size than its analogues C-152 and C-481 or other rigid molecules, it may occupy different positions in the Stern layer from other dyes. This is illustrated in Scheme 3. According to Scheme 3, C-151, being smaller in size, likes to penetrate into the deeper side of the Stern layer. It is easy to understand that, due to having a smaller size than other acceptor molecules, C-151 resides in a close proximity to the headgroups of the surfactant. It is well-known that reactants attached to the headgroups of the surfactant molecules will experience a more restricted environment than faced by the molecules away from the surfactant headgroups. Moreover, C-151 is strongly nucleated by those solvent molecules, which are attached to the surfactant headgroups. Thus, by all of these effects, C-151 experiences a more constrained environment than other coumarin dyes; hence, it shows a slower rotational relaxation as well as a slower translatioanl diffusion motion compared to other dyes. The translation diffusion coefficients for C-151 in SDS micelles and in BSA−SDS complexes are 9.54 and 6.5 cm^2/s, respectively, while for C-152 the translation diffusion coefficients are 24.4 and 14 cm^2/s, respectively, and for C-481 these values are 23 and 10 cm^2/s, respectively. The slower translational diffusion of C-151 may be responsible for the slower intermolecular electron transfer, although direct correlation between the translational diffusion coefficients and fluorescence quenching rate constants is not possible in the present case. However, in the present work, an interesting observation is that both translational diffusion coefficients and fluorescence quenching electron transfer rate constants of C-151 in SDS micelles and in BSA−SDS complexes are smaller than those of C-152 and C-481 by approximately a factor of 2. This is what we observed in Figure 5. Therefore, the observed variation in the electron transfer rate at the higher free energy region may be a consequence of different translation diffusion coefficients of the coumarin dyes along the micellar surface. Another possibility is that a slight change in donor−acceptor distance (even by 1 Å) affects the rate markedly (since the rate varies exponentially with the distance). Scheme 3 also suggests that C-151 will be less accessible to the DMA molecules than C-152 and C-481 due to the different locations. As electron transfer is governed by the spatial distribution of the acceptor around the excited dye, a less accessible acceptor (C-151 in the present case) may show retardation in the electron transfer rate. It is also possible that the different positions of C-151 (Scheme 3) and higher nucleation by the solvent molecules and bonding to the surfactant headgroups may give rise to a sterically hindered coumarin−amine encounter complex, causing retardation in the electron transfer rate.

4. Conclusion

In the present work, the photoinduced fluorescence quenching electron transfer rate is found to be slower in BSA−SDS protein−surfactant complexes compared to that in SDS micelles. The slower electron transfer dynamics in BSA−SDS protein−surfactant complexes is supposed to be arising due to the necklace-and-bead structure of BSA−SDS complexes. The slower solvation dynamics and slower rotational relaxation studies also indicate that probe molecules experience a more confined environment due to the formation of a necklace-and-bead structure by the interaction between protein and surfactant molecules. The correlation of free energy change to the fluorescence quenching electron transfer rate reveals a deviation from the normal Marcus region by showing retardation in the electron transfer rate of coumarin 151. This observation is attributed to the slower rotational relaxation and slower translational diffusion of C-151 compared to C-152 and C-481 in the micelles and protein−surfactant complexes. The slower rotational relaxation and slower transnational diffusion of C-151 compared to C-152 and C-481 are the consequences of the stronger attachment of C-151 to the solvent molecules and the headgroup region in the micelles.

Acknowledgment. N.S. is thankful to Department of Science and Technology (DST), Government of India, for a generous research grant. A.C., D.S., and P.S. are thankful to CSIR for research fellowships. We are thankful to an anonymous reviewer for pointing out the hydrophobicities of C-151 and DMA. Thanks to Dr. Samir Kumar Pal of S.N. Bose National Centre for Basic Sciences for allowing us to use the spectrofluorimeter.

References and Notes

(1) Dickinson, E. Protein in solution and interfaces. In *Interaction of Surfactants with Polymers and Proteins*; Goddard, E. D., Ananthapadmanabhan, K. P., Eds.; CRC Press: London, 1993; Chapter 7, p 295.

(2) Schwuger, M. J.; Bartnik, F. G. In *Anionic Surfactants*; Gloxhuber, C., Ed.; Surfactant Science Series, Vol. 10; Marcel Dekker: New York, 1980; Chapter 1.

(3) Jones, M. N. *Chem. Soc. Rev.* **1992**, *21*, 127.

(4) Turro, N. J.; Lei, X.-G.; Ananthapadmanabhan, K. P.; Aronson, M. *Langmuir* **1995**, *11*, 2525.

(5) Takeda, K.; Hachiya, K.; Moriyama, Y. *Interaction of Protein with Ionic Surfactants: Part 1*; Marcel Dekker: New York, 2002; p 2558.

(6) Takeda, K.; Hachiya, K.; Moriyama, Y. *Interaction of Protein with Ionic Surfactants: Part 2*; Marcel Dekker: New York, 2002; p 2575.

(7) Kelley, D.; McClements, D. J. *Food Hydrocolloids* **2003**, *17*, 73.

(8) Peters, T. J. *All About Albumin Biochemistry, Genetics, and Medical Applications*; Academic Press: San Diego, CA, 1996.

(9) Foster, J. F. In *Albumin Structure, Function and Uses*; Rosenoer, V. M., Oratz, M., Rothschild, M. A., Eds.; Pergamon Press Inc.: Oxford, U.K., 1977; pp 53−84.

(10) Vijai, K.; Forster, J. *Biochemistry* **1967**, *6*, 1152. Curry, S.; Mandelkow, H.; Brickm, P.; Franks, N. *Nat. Struct. Biol.* **1998**, *5*, 827.

(11) Curry S.; Mandelkow, H.; Brick, P.; Franks, N. *Nat. Struct. Biol.* **1998**, *5*, 827.

(12) Oakes, J. *J. Chem. Soc., Faraday Trans. 1* **1974**, *70*, 2200.

(13) Moren, A. K.; Nyden, M.; Soderman, O.; Khan, A. *Langmuir* **1995**, *11*, 5480.

(14) Valstar, A.; Almgren, M.; Brown, W.; Vasilescu, M. *Langmuir* **2000**, *16*, 922.

(15) Takeda, K.; Sasaoka, H.; Sasa, K.; Hirai, H.; Hachiya, K.; Moriyama, Y. *J. Colloid Interface Sci.* **1992**, *154*, 385.

(16) Valstar, A.; Vasilescu, M.; Vigouroux, C.; Stilbs, P.; Almgren, M. *Langmuir* **2001**, *17*, 3208.

(17) Gimel, J. C.; Brown, W. *J. Chem. Phys.* **1996**, *104*, 8112.

(18) Guo, X. H.; Zhao, N. M.; Chen, S. H.; Teixeira, J. *Biopolymers* **1990**, *29*, 335.

(19) Ibel, K.; May, R. P.; Kirschner, K.; Szadkowski, H.; Mascher, E.; Lundahl, P. *Eur. J. Biochem.* **1990**, *190*, 311.

(20) Vasilescu, M.; Angelescu, D.; Almgren, M.; Valstar, A. *Langmuir* **1999**, *15*, 2635.

(21) Gelamo, E. L.; Silva, C. H. T. P.; Imasato, H.; Tabak, M. *Biochim. Biophys. Acta* **2002**, *1594*, 84.

(22) Gelamo, E. L.; Tabak, M. *Spectrochim. Acta, Part A* **2000**, *56*, 2255.

(23) Hazra, P.; Chakrabarty, D.; Chakraborty, A.; Sarkar, N. *Biochem. Biophys. Res. Commun.* **2004**, *314*, 543.

(24) Mukherjee, S.; Sen, P.; Halder, A.; Sen, S.; Dutta, P.; Bhattacharyya, K. *Chem. Phys. Lett.* **2003**, *379*, 471.

(25) Dutta, P.; Sen, P.; Halder, A.; Mukherjee, S.; Sen, S.; Bhattacharyya, K. *Chem. Phys. Lett.* **2003**, *377*, 229.

(26) Bhattacharyya, K. *Acc. Chem Res.* **2003**, *36*, 95.

(27) Kobayashi, T.; Takagi, Y.; Kandori, H.; Kemnitz, K.; Yoshihara, K. *Chem. Phys. Lett.* **1991**, *180*, 416.

(28) Yartsev, A.; Nagasawa, Y.; Douhal, A.; Yoshihara, K. *Chem. Phys. Lett.* **1993**, *207*, 546.

(29) Rubstov, I. V.; Shirota, H.; Yoshihara, K. *J. Phys. Chem.* **1999**, *103*, 1801.
(30) Kandori, H.; Kemnitz, H.; Yoshihara, K. *J. Phys. Chem.* **1992**, *96*, 8042.
(31) Yoshihara, K.; Nagasawa, Y.; Yartsev, A.; Kumazaki, S.; Kandori, H.; Johnsin, A. E.; Tominaga, K. *J. Photochem. Photobiol., A* **1994**, *80*, 169.
(32) Engleitner, S.; Seel, M.; Zinth, W. *J. Phys. Chem. A* **1999**, *103*, 3013.
(33) Seel, M.; Engleitner, S.; Zinth, W. *Chem. Phys. Lett.* **1993**, *275*, 363.
(34) Shirota, H.; Pal, H.; Tominaga, K.; Yoshihara, K. *J. Phys. Chem. A* **1998**, *102*, 3089.
(35) Yoshihara, K.; Tominaga, K.; Nagasawa, Y. *Bull. Chem. Soc. Jpn.* **1995**, *68*, 696 and references therein.
(36) Castner, E. W., Jr.; Kennedy, D.; Cave, R. J. *J. Phys. Chem. A* **2000**, *104*, 2869.
(37) Nagasawa, Y.; Yartsev, A. P.; Tominaga, K.; Bisht, P. B.; Johnson, A. E.; Yoshihara, K. *J. Phys. Chem*. **1995**, *99*, 653.
(38) Shirota, H.; Pal, H.; Tominaga, K.; Yoshihara, K. *Chem. Phys.* **1998**, *236*, 355.
(39) Pal, H.; Nagasawa, Y.; Tominaga, K.; Yoshihara, K. *J. Phys. Chem.* **1996**, *100*, 11964.
(40) Pal, H.; Shirota, H.; Tominaga, K.; Yoshihara, K. *J. Chem. Phys.* **1999**, *110*, 11454.
(41) Wang, C.; Akhremitchev, B.; Walker, G. C. *J. Phys. Chem. A* **1997**, *101*, 2735.
(42) Mcarthur, E. A.; Eisenthal, K. B. *J. Am. Chem. Soc.* **2006**, *128*, 1068.
(43) Marcus, R. A. *J. Chem. Phys.* **1956**, *24*, 966.
(44) *Electron Transfer from Isolated Molecules to Biomolecules*; Jortner, J., Bixon, M., Eds.; Advances in Chemical Physics Parts 1 & 2, Vols. 1067 and 107; Wiley: New York, 1999.
(45) Marcus, R. A.; Sutin, N. *Biochim. Biophys. Acta* **1985**, *811*, 265.
(46) Chakraborty, A.; Chakrabarty, D.; Hazra, P.; Seth, D.; Sarkar, N. *Chem. Phys. Lett.* **2003**, *382*, 508.
(47) Chakraborty, A.; Chakrabarty, D.; Seth, D.; Hazra, P.; Sarkar, N. *Spectrochim. Acta, Part A* **2006**, *63*, 594.
(48) Chakraborty, A.; Chakrabarty, D.; Seth, D.; Hazra, P.; Sarkar, N. *Chem. Phys. Lett.* **2005**, *18*, 405.
(49) Kumbhakar, M.; Nath, S.; Pal, H.; Sapre, A. V.; Mukherjee, T. *J. Chem. Phys.* **2003**, *119*, 388.
(50) Kumbhakar, M.; Mukherjee, T.; Pal, H. *Chem. Phys. Lett.* **2005**, *410*, 94.
(51) Kumbhakar, M.; Nath, S.; Mukherjee, T.; Pal, H. *J. Chem. Phys.* **2005**, *123*, 34705.
(52) Chakraborty, A.; Seth, D.; Setua, P.; Sarkar, N. *J. Chem. Phys.* **2006**, *124*, 74512.
(53) Frauchiger, L.; Shirota, H.; Uhrich K. E.; Castner, E. W., Jr. *J. Phys. Chem. B* **2002**, *106*, 7463.
(54) Shirota, H.; Tamoto, Y.; Segawa, H. *J. Phys. Chem. A* **2004**, *108*, 3244.
(55) Quitevis, E. L.; Marcus, A. H.; Fayer, M. D. *J. Phys. Chem.* **1993**, *97*, 5762.
(56) Krishna, M. M. G.; Das, R.; Periasamy, N.; Nityananda, R. *J. Chem. Phys.* **2000**, *112*, 8502.
(57) Sen, S.; Sukul, D.; Dutta, P.; Bhattacharyya, K. *J. Phys. Chem. A* **2001**, *105*, 7495.
(58) Maiti, N. C.; Krishna, M. M. G.; Britto, P. J.; Periasamy, N. *J. Phys. Chem. B* **1997**, *101*, 11051.
(59) Dutt, G. B. *J. Phys. Chem. B* **2003**, *107*, 10546.
(60) Pal, S. K.; Mandal, D.; Sukul D.; Bhattacharyya, K. *Chem. Phys.* **1999**, *249*, 63.
(61) Berr, S. S. *J. Phys. Chem*. **1987**, *91*, 4760.
(62) Berr, S. S.; Coleman, M. J.; Jones, R. R. M., Jr.; Johnson J. S. *J. Phys. Chem.* **1986**, *90*, 6492.
(63) Nad, S.; Pal, H. *J. Phys. Chem. A* **2000**, *104*, 673.
(64) Mazumdar, M.; Parrack, P. K.; Bhattacharyya, B. *Eur. J. Biochem.* **1992**, *204*, 127.
(65) Sarkar, N.; Datta, A.; Das, S.; Bhattacharyya, K. *J. Phys. Chem.* **1996**, *100*, 15483.
(66) Tamoto, Y.; Segawa, H.; Shirota, H. *Langmuir* **2005**, *21*, 3757.
(67) Pal, S. K.; Sukul, D.; Mandal, D.; Sen, S.; Bhattacharyya, K. *Chem. Phys. Lett.* **2000**, *327*, 91.
(68) Hara, K.; Baden, N.; Kajimoto, O. *J. Phys.: Condens. Matter* **2004**, *16*, S1207.
(69) Edward, J. T. *J. Chem. Educ.* **1970**, *47*, 261.
(70) Miller, J. R.; Calcaterra, L. T.; Closs, G. L. *J. Am. Chem. Soc.* **1984**, *106*, 3047.
(71) Closs, G. L.; Miller, J. R. *Science* **1988**, *240*, 440.
(72) Fox, L. S.; Kozik, M.; Winulr, J. R.; Gray, H. B. *Science* **1990**, *247*, 1069.
(73) Gould, I. R.; Farid, S. *Acc. Chem. Res.* **1996**, *29*, 522.
(74) Fukuzumi, S.; Ohkubo, K.; Imahori, H.; Guldi, D. M. *Chem.—Eur. J.* **2003**, *9*, 1585.
(75) Turro, C.; Zalesky, J. M.; Karabatsos, Y. M.; Nocera, D. G. *J. Am. Chem. Soc.* **1996**, *118*, 6060.
(76) Prasad, E.; Gopidas, K. R. *J. Am. Chem. Soc.* **2000**, *122*, 3191.
(77) Smitha, M. A.; Prasad, E.; Gopidas, K. R. *J. Am. Chem. Soc.* **2001**, *123*, 1159.
(78) Weidernair, K.; Tavenier, H. L.; Fayer, M. D. *J. Phys. Chem. B* **1997**, *101*, 9352.
(79) Tavernier, H. L.; Barzykin, A. V.; Tachiya, M.; Fayer, M. D. *J. Phys. Chem. B* **1998**, *102*, 6078.
(80) Kim, T. G.; Topp, M. R. *J. Phys. Chem. A* **2004**, *108*, 7653.
(81) Das, K.; Jain, Gupta, P. K. *Chem. Phys. Lett.* **2005**, *410*, 160.